JVI Accepted Manuscript Posted Online 28 April 2021
J Virol doi:10.1128/JVI.02374-20

Inhibitors of coronavirus 3CL proteases protect cells from protease-mediated cytotoxicity

Samuel J. Resnick[1,2], Sho Iketani[3,4], Seo Jung Hong[1], Arie Zask[5], Hengrui Liu[6], Sungsoo Kim[1], Schuyler Melore[1], Fang-Yu Lin[7], Manoj S. Nair[3], Yaoxing Huang[3], Sumin Lee[6], Nicholas E.S. Tay[6], Tomislav Rovis[6], Hee Won Yang[1], Li Xing[7], Brent R. Stockwell[5,6*], David D. Ho[3*], Alejandro Chavez[1*]

[1] Department of Pathology and Cell Biology, Columbia University Irving Medical Center, New York, NY, 10032, USA

[2] Medical Scientist Training Program, Columbia University Irving Medical Center, New York, NY, 10032, USA

[3] Aaron Diamond AIDS Research Center, Columbia University Irving Medical Center, New York, NY, 10032, USA

[4] Department of Microbiology and Immunology, Columbia University Irving Medical Center, New York, NY, 10032, USA

[5] Department of Biological Sciences, Columbia University, New York, NY, 10027, USA

[6] Department of Chemistry, Columbia University, New York, NY, 10027, USA

[7] WuXi AppTec, Cambridge, MA 02142, USA

***Correspondence:** ac4304@cumc.columbia.edu; dh2994@cumc.columbia.edu; bstockwell@columbia.edu

Abstract

We describe a mammalian cell-based assay to identify coronavirus 3CL protease (3CLpro) inhibitors. This assay is based on rescuing protease-mediated cytotoxicity and does not require live virus. By enabling the facile testing of compounds across a range of 15 distantly related coronavirus 3CLpro enzymes, we identify compounds with broad 3CLpro inhibitory activity. We also adapt the assay for use in compound screening and in doing so uncover additional SARS-CoV-2 3CLpro inhibitors. We observe strong concordance between data emerging from this assay and those obtained from live virus testing. The reported approach democratizes the testing of 3CLpro inhibitors by developing a simplified method for identifying coronavirus 3CLpro inhibitors that can be used by the majority of laboratories, rather than the few with extensive biosafety infrastructure. We identify two lead compounds, GC376 and compound 4, with broad activity against all 3CL proteases tested including 3CLpro enzymes from understudied zoonotic coronaviruses.

Importance

Multiple coronavirus pandemics have occurred over the last two decades. This has highlighted a need to be proactive in the development of therapeutics that can be readily deployed in the case of future coronavirus pandemics. We develop and validate a simplified cell-based assay for the identification of chemical inhibitors of 3CL proteases encoded by a wide range of coronaviruses. This assay is reporter-free, does not require specialized biocontainment, and is optimized for performance in high-throughput screening. By testing reported 3CL protease inhibitors against a large collection of 3CL proteases with variable sequence similarity, we identify compounds with broad activity against 3CL proteases and uncover structural insights that contribute to their broad activity. Furthermore, we demonstrate this assay is suitable for identifying chemical inhibitors of proteases from families other than 3CL proteases.

Introduction

The outbreak of a novel coronavirus (SARS-CoV-2) infection has paralyzed countries around the world [1,2]. This crisis is further exacerbated by the dearth of approved therapeutics, leaving physicians with few proven treatment options. In the past two decades, the world has suffered from two other major coronavirus outbreaks, Severe Acute Respiratory Syndrome (SARS) and Middle East Respiratory Syndrome (MERS), suggesting that coronaviruses represent a real and ever-present threat to global health that must be addressed [3]. Yet, even if therapeutics against the existing epidemic strains are identified, there are several hundred other coronaviruses in active circulation within animal populations, many of which are understudied, but have the theoretical potential to infect humans. To help identify therapeutics for the current epidemic along with preparing for the next, there is a need for readily-deployable small molecule screening assays that enable the identification of therapeutics that are broad-acting across a large collection of coronavirus strains.

During coronavirus infection, the RNA genome is delivered into cells and translated into a pair of polyproteins [4]. These polyproteins are then processed by a set of virally encoded proteases, of which the three-chymotrypsin-like protease (3CLpro) performs the majority of cleavage events [4]. As a result of its essential role in viral replication and high degree of conservation across all coronaviruses, 3CLpro enzymes represent important targets for therapeutic drug development [5,6]. Previous work expressing a variety of viral proteases within yeast and mammalian cells have shown that protease expression can lead to cellular toxicity, which can be rescued by the addition of protease inhibitors [7-13]. We hypothesized that the expression of coronavirus 3CLpro enzymes within mammalian cells may lead to a similar toxic phenotype as a result of its proteolytic activity. If 3CL protease inhibitors rescue the toxic phenotype, this could form the basis of a cell-based assay to detect 3CL protease inhibitors. While multiple assays exist for evaluating protease inhibitors, an assay of the nature has clear advantages, as it requires minimal upfront cost or effort, is accessible to many biomedical research labs, does not involve the use of live virus, and requires no specialized reporter to read out protease activity. In contrast, *in vitro* protease assays using purified protein have formed the backbone of inhibitor screening, but require upfront efforts to isolate the pure protease and are not conducted under physiologic cellular conditions [14,15]. In addition, if one desires to identify broad-acting coronavirus inhibitors, one must purify and identify experimental conditions suitable for testing each protease *in vitro*. An alternative approach for identifying protease inhibitors is the use of live virus which is performed under more biologically relevant conditions, assuming relevant host cell systems can be identified, but requires intensive safety training and specialized biosafety protocols [16]. In addition, for many coronaviruses, no live virus assay exists, limiting the ability to test compounds within mammalian cell systems to a small subset of all coronaviruses [17]. Furthermore, compounds with activity against live virus may function through a number of mechanisms other than 3CLpro inhibition which cannot be readily

determined when performing the assay, and may lead to undesired off-target activities which are not realized until much later in the drug development process [18,19].

Here, we report a mammalian cell-based assay for identifying coronavirus 3CLpro inhibitors that does not require the use of live virus. We demonstrate the utility of the assay by characterizing a variety of SARS-CoV-2 3CLpro inhibitors and obtaining EC_{50} values that are highly concordant with the results from live virus testing. We then establish the generality of our approach across a diverse set of 15 3CLpros from a wide range of coronaviruses, and in doing so identify a set of key structural features shared among broadly active 3CLpro inhibitors. We next perform a small molecule screen, along with structure-activity profiling of a set of compounds to find those with enhanced antiviral activity. Finally, we provide data that suggest our approach is applicable to other protease families and thus represents a general platform for viral protease inhibitor studies.

Results

Expression of the SARS-CoV-2 3CLpro in HEK293T cells results in protease-mediated cytotoxicity that can be rescued by protease inhibitors

Motivated by prior work demonstrating protease-mediated cytotoxicity, we sought to determine the effect of transfecting an expression plasmid encoding the SARS-CoV-2 3CLpro into HEK293T cells. Utilizing a cost-effective crystal-violet-based approach to quantify cell abundance, we observed that SARS-CoV-2 3CLpro expression results in significant growth inhibition as compared to a control construct containing enhanced yellow fluorescent protein (EYFP) (Fig. 1a-b) [20]. This suppression of growth was dependent upon the catalytic function of the enzyme, as mutating cysteine 145, which is essential for the enzyme's proteolytic activity, abolished the growth defect (Fig. 1a-b). We confirmed expression of active and inactive SARS-CoV-2 3CLpro enzymes in HEK293T cells with western blotting (Fig 1c). We next determined if the observed growth defect could be rescued by incubating cells with GC376, a previously reported SARS-CoV-2 3CLpro inhibitor [21]. In comparison to untreated control cells, the addition of GC376 led to a robust increase in cell growth (Fig. 1d-e). To ensure reproducibility between transfections and to select for cells expressing 3CL protease, expression constructs contained a puromycin resistance marker and puromycin resistance was selected for 24 h after transfection.

Compound rescue of transfected 3CLpro cytotoxicity mimics the results obtained with live virus

We next tested if this transfection-based assay could be used to determine compound EC_{50} values and whether the values showed any correlation with those obtained with live virus assays. After incubating SARS-CoV-2 3CLpro transfected cells with a range of GC376 concentrations, we calculated an EC_{50} of 3.30 μM, which is similar to published values using live virus on Vero E6 cells (EC_{50} 4.48 μM, 3.37 μM, 2.2 μM, 0.9 μM, 0.18 μM) (Fig. 2a and Table 1) [21-26]. We then investigated the assay's tolerance to deviation by

varying the amount of plasmid transfected or the number of cells seeded into wells containing compound (Supplementary Fig. 1). In all cases, the assay was robust to variation, delivering a similar EC_{50} for GC376 across all conditions. We also tested an orthogonal method of quantifying cell abundance based on fluorescence microscopy and observed agreement with the results obtained with crystal violet staining (Supplementary Fig. 2). In the fluorescence microscopy approach, EYFP labeled cells are transfected with the SARS-CoV-2 3CLpro expression construct. Rather than reading out the cellular abundance using crystal violet staining, the area occupied by the cells under various treatment conditions is measured with a fluorescent microscope. As a whole these data suggest that our approach provides consistent results across methods of measurement, although with the crystal violet assay we observed lower measurement variability and higher changes in relative growth and thus, the crystal violet approach was chosen for further validation.

We next conducted dose-response profiling for two additional SARS-CoV-2 3CLpro inhibitors, compound 4 and 11a, and observed reversal of the toxic effect of the protease in a dose-dependent manner (Fig. 2b-c) [27,28]. In agreement with the results obtained with GC376, the EC_{50} value for compound 4 was comparable to those obtained with live virus, 0.98 µM and 3.023 µM, respectively (Table 1) [24]. Unexpectedly, we calculated an EC_{50} of 6.89 µM for 11a, which is approximately 10-fold higher than the literature reported value of 0.53 µM, based on viral plaque assay [27]. We have noticed that literature reported EC_{50} values from live virus testing can show over an order of magnitude difference in the reported EC_{50} values depending on the exact method employed, as is the case for GC376 (Table 1). To resolve the discrepancy between the transfection-based approach and the live virus assay for 11a, we conducted live virus testing of 11a using the commonly employed readout of protection from cytopathic effect (CPE) in Vero E6 cells and observed closer concordance with our transfection-based results, with a reported EC_{50} of 3.83 µM (Supplementary Fig. 3 and Table 1) [21,24,29]. During the course of our studies, we also measured the toxicity of each compound by exposing EYFP-transfected cells to each molecule and determining CC_{50} values (Fig. 2). Using these data, we calculated the selectivity index (SI) for each compound, observing that both GC376 and compound 4 show moderate selectivity (SI > 10) for SARS-CoV-2 (Supplementary Table 1).

As our assay requires that inhibitors successfully engage their protease target within the intracellular milieu, we hypothesized that it would be able to distinguish between compounds that are only active on the *in vitro* purified SARS-CoV-2 3CLpro and those that inhibit viral replication by blocking 3CLpro activity *in situ*. In general, we observe concordance between compounds showing activity within this transfection-based 3CLpro assay and live virus studies (Supplementary Fig. 4a-e) [14,30]. However, within our assay we did not observe activity for ebselen, a small molecule with demonstrated *in vitro* activity against purified SARS-CoV-2 3CLpro and data showing inhibition of SARS-CoV-2 live virus (Supplementary Fig. 4f). We suggest that this may be due to ebselen targeting more than 3CLpro within the live virus assay, which is in line with

Journal of Virology

reports showing that ebselen is highly reactive and readily forms selenosulfide bonds with numerous proteins including the SARS-CoV-2 papain-like protease (PLP) [19,31-33].

Assay is applicable to a range of coronavirus 3CLpro enzymes

We next sought to determine if our simplified testing paradigm could be used to study other coronavirus 3CLpros, to enable users to identify broad-acting compounds. To test the assay's generality, we created expression constructs for 3CL proteases from five other coronaviruses (SARS-CoV, MERS-CoV, Bat-CoV-HKU9, HCoV-NL63 and IBV) with variable amino acid identity compared with SARS-CoV-2 3CLpro (Supplementary Fig. 5a). For each of these proteases, we confirmed that expression in mammalian cells resulted in toxicity that is dependent upon the enzyme's catalytic activity (Supplementary Fig. 5b). We also observed expression of each construct by western blot (Supplementary Fig. 5c). Next, we tested GC376, compound 4, and 11a across this panel of proteases. GC376, a drug originally identified for use against the Feline Infectious Peritonitis virus, showed EC_{50} <10 μM for most, but not all of proteases tested [34]. Unexpectedly, compound 4, which was originally designed as a SARS-CoV 3CLpro inhibitor showed particular potency against IBV 3CLpro (EC_{50} = 0.058 μM) along with broad activity (EC_{50} <10 μM) for all other 3CL proteases tested. In contrast to GC376 and compound 4, 11a had a relatively narrow activity spectrum with EC_{50} <10 μM against only SARS-CoV and SARS-CoV-2 3CLpro enzymes (Fig. 3). Of note, in all cases where previous live virus data was available, the EC_{50} values obtained from this transfection-based assay were similar (Table 1).

Differences in the 3CLpro S2 pocket explain variable susceptibility to 11a

Given similarities between 11a and our other tested inhibitors, we were intrigued by its narrow spectrum of activity and sought to uncover the mechanism underlying this observation. In examining published crystal structures, we observed striking variability in the S2 pocket between 3CLpros, with some having large, flexible, and nonpolar S2 pockets (e.g. SARS and SARS-CoV-2) and others showing narrower, less flexible, and more polar S2 pockets (e.g. MERS-CoV, IBV, and HCoV-NL63) (Fig 4a-b and Supplementary Fig. 6). We hypothesized these differences in the S2 pocket explain why 11a, with its larger cyclohexylmethyl P2 group which interacts with the S2 pocket, is unable to potently inhibit the majority of tested 3CLpros. In contrast, GC376 and compound 4 both have a smaller isobutyl P2 group and are less restricted by differences in the S2 pocket, and are able to interact with a larger number of 3CLpros. To test this hypothesis, we took the broadly activity inhibitor, GC376, and synthesized an analog, SL-4-241, which substitutes the isobutyl P2 group for the bulkier cyclohexylmethyl moiety from 11a (Fig. 4c). When tested against SARS and MERS 3CLpros, SL-4-241 only showed activity against SARS-CoV-2 with its more accommodating S2 pocket (Fig. 4d-e). These data suggest that broad acting inhibitors should avoid the use of bulky P2 groups, as these will limit their activity to only a small subset of all 3CLpros.

Rapid testing of protease inhibitors elucidates structure-function relationships

Having demonstrated the assay's performance when testing individual compounds, we sought to determine its suitability for small molecule screening. Before performing the screen, we optimized the testing parameters to ensure suitable performance characteristics (Supplementary Fig. 7 and Methods) [35]. We compiled a collection of 162 diverse protease inhibitors, along with compounds with reported *in vitro* activity against 3CLpro enzymes or structural similarity to known 3CLpro inhibitors (Supplementary Table 2 and Supplementary Table 3). Of the nearly 200 compounds tested against the SARS-CoV-2 3CLpro, two potent hits were identified, GC373 and GRL-0496 (Fig. 5a, Supplementary Table 2) [36]. Also included in the compounds screened were several apoptosis inhibitors. Notably, we did not call hits for these compounds which suggests that apoptosis inhibitors do not give false positive results in our assay (Supplementary Table 2).

Our first hit, GC373, is structurally similar to its prodrug GC376, except for the change of the bisulfite salt adduct to an aldehyde warhead [26,37]. Additional testing of GC373 revealed it to have a similar EC_{50} as GC376 across a range of 3CLpros within our transfection-based assay and when tested against live SARS-CoV-2 virus, suggesting that the difference in structure has a minimal effect on potency (Supplementary Fig. 8 & 9 and Table 1), although solubility may be affected [37]. The other hit from the screen, GRL-0496 was further tested and was found to have an EC_{50} of 5.05 μM against SARS-CoV-2 3CLpro in our transfection-based assay (Fig. 5c). To verify GRL-0496's activity, we tested it against live SARS-CoV-2 virus, and confirmed its potency (EC_{50} = 9.12 μM) (Fig. 5d). We next tested GRL-0496 against the full panel of 3CLpro enzymes we previously examined and observed a narrow range of activity, with EC_{50} <10 μM only observed against SARS-CoV 3CLpro and SARS-CoV-2 3CLpro, in agreement with previous live virus testing (Supplementary Fig. 9 and Table 1) [29].

Further analysis of the screened compounds revealed a large number that were structurally similar to GRL-0496, with one being a previously reported 3CLpro inhibitor (MAC-5576) that failed to show activity within our transfection-based assay, in agreement with recent live virus studies (Fig. 5b) [24,38]. We hypothesize that the difference in activity between these compounds is due to the indole group in GRL-0496 forming a more stable inhibitory thioester bond with the 3CLpro catalytic cysteine as compared to the more unstable thioester bonds formed by MAC-5576, BTB07408, and BTB07417 (see Supplementary Note 1 for further discussion).

Further testing against 3CLpros confirms a pair of broadly active lead compounds

Two compounds from our studies, GC376 and compound 4, demonstrated activity across the six 3CLpros tested and also harbor small P2 substituents that may be less likely to restrict target engagement. To further characterize the extent to which these two compounds may serve as valuable lead candidates, we tested

them against 3CLpros from nine other coronavirus species. For these additional studies, we focused mostly on testing additional members from the betacoronavirus and alphacoronavirus lineages, as these are the genera which are known to infect humans. Within these genera, many coronaviruses have no established live virus assay to enable small molecule testing. We validated that expression of these 3CLpros within HEK293T cells results in protease-mediated cytotoxicity dependent upon the enzyme's catalytic function (Supplementary Fig. 10). Next, we conducted dose-response curves with GC376 and compound 4 for each of these additional 3CLpros. Both compounds demonstrated activity against all additional 3CLpros tested (Fig. 6). Compound 4 had an EC_{50} of <10 μM for 13/15 3CLpros while GC376 had an EC_{50} of <10 μM for 12/15 3CLpros, suggesting that these compounds represent promising leads capable of inhibiting 3CLpro within a wide range of coronaviruses including zoonotic coronaviruses with the potential to transmit to humans.

Expansion of assay to other protease families

Having established the power of our assay to rapidly characterize 3CLpros inhibitors, we sought to explore whether our approach was generalizable for other protease families. We expressed the 3C protease from Human Rhinovirus B14 (HRV-B14 3C) and the SARS-CoV papain-like protease (SARS-CoV PLP) within HEK293T cells as both of these proteases are well characterized with documented small molecule inhibitors tested in live virus assays. In cells transfected with the protease containing constructs, we observed marked cytotoxicity and a dose-dependent reversal of toxicity when cells were incubated with either a known 3C protease or PLP inhibitor, respectively (Supplementary Figure 11). As with our 3CLpro studies, the EC_{50} values obtained from our transfection-based approach showed excellent concordance with live virus studies for both of these proteases, suggesting that our approach to compound testing may be generalizable to many other protease families (Table 1) [39-41].

Discussion

Given the essentiality of the coronavirus 3CL protease for viral replication and the success of protease inhibitors in the treatment of viral illness, the chemical inhibition of coronavirus 3CL proteases represent a promising avenue for treating infections caused by this large family of viruses. Here, we present a simplified assay to identify and characterize candidate inhibitors under physiologic cellular conditions. While conventional methods for identifying 3CL protease inhibitors make use of *in vitro* purified protease, the isolation of sufficiently pure enzyme in its native state can be costly and labor intensive. Furthermore, assays using purified protease fail to consider cell permeability and the influence of the extracellular and intracellular milieu on compound activity. In contrast, live virus-based assay are performed under physiologically relevant conditions but require extensive biosafety containment while many coronaviruses, particularly those of zoonotic origin, do not have existing live virus assays [42,43]. In comparison, our approach presents significant advantages over these traditional approaches, given its physiologic relevance

and ability to be performed with equipment, reagents, and safety infrastructure commonly available to the majority of biomedical research laboratories. The phenotype assayed within our approach is driven solely by protease activity, and thus it is not subject to the same confounders as live virus assays. In live virus assays, a tested compound may function against multiple cellular targets to inhibit viral replication, which has been demonstrated for 3CLpro inhibitors that are also active against Cathepsin L, an endopeptidase with a role in SARS-CoV-2 replication [19,21,44]. Generally toxic compounds may also result in observed activity during live virus assays as a result of cellular perturbations that prevent viral replication [45]. Additionally, cell line specific effects of live virus assays have been observed, most notably for hydroxychloroquine, wherein compounds may inhibit viral replication in certain cell lines but are not active in other cell lines [46]. These properties of live virus assays may complicate drug screening results and lead to uncertainty about compound mechanism. In contrast, our approach allows users to identify compounds whose function is squarely dependent on 3CLpro inhibition and may be less likely to demonstrate off-target activity during further development or when tested in the live virus setting. Other 3CL protease cell-based assays have also been developed, such as the FlipGFP and pGlo assays, which are based on reporters that become fluorescent or can activate luminescence when cut by the 3CL protease, respectively [22,47,48]. Our approach performs similarly to these assays wherein the FlipGFP assay reports an EC_{50} of 5.5 μM for the interaction between GC376 and SARS-CoV-2 3CL in comparison to our reported EC_{50} of 3.30 μM. The pGlo assay has reported an EC_{50}s of 2.68 μM and 3.41 μM for the interaction between GRL-0496 and SARS-CoV 3CLpro and SARS-CoV-2 3CLpro, respectively, which are in line with our reported values of 7.84 μM and 5.05 μM. With similar performance, our assay provides advantages over these cell-based assays in that it has been extensively validated across 3CL proteases and a wide range of compounds, has been optimized for high-throughput screening, and does not require reporters to be modified when testing different proteases.

Within the literature, EC_{50} values obtained for a 3CLpro inhibitor against live virus can show a broad range of reported potencies, with EC_{50} values at times ranging across multiple orders of magnitude (Table 1). These differences appear to be driven by variation in experimental setup such as cell line used, assay readout, incubation period, and initial concentration of virus added. While we have observed agreement between the EC_{50} values obtained from the described transfection-based method and those reported in the literature, given the differences in EC_{50} across assays, we suggest caution when comparing results across studies. By developing this transfection-based 3CLpro testing platform, we hope to facilitate the discovery of new coronavirus inhibitors while also facilitating the comparison of existing inhibitors within a single simplified assay system. Furthermore, we propose that this cellular protease assay system could be industrialized to screen and optimize a large number of compounds to discover potential treatments for future viral pandemics.

During our studies, we observed protease-mediated cytotoxicity and small molecule rescue for 15 3CLpros, suggesting that our assay is widely applicable to this family of proteases. The plasticity of the assay across various 3CLpros is of particular significance given the myriad of coronaviruses that have no live virus assay and therefore have few options available for testing compound efficacy within mammalian cells. The approach is also compatible with small molecule screening and allows for comparisons across 3CLpros to obtain structural insights into compound activity such as our studies of 11a, GC376, and SL-4-241 that demonstrated the role of the P2 substituent in dictating compound specificity.

Our findings have important implications for the manner in which small molecule protease inhibitors are studied. We propose that given our assay's breadth and ease of use it is well suited to form the backbone of a forward-thinking pandemic preparedness strategy. The goal of such a strategy would be the proactive identification of inhibitors capable of addressing not only the current human coronaviral strains, but also small molecule leads against zoonotic strains with the highest potential to transmit into humans. Such a strategy if properly implemented would provide the biomedical community with a series of high value chemical leads upon which to perform additional focused chemical optimization or if already passed through preclinical testing a set of compounds ready for rapid translation into humans.

Materials and Methods

Cell Lines and Cell Culture

HEK293T and HEK293 cells used in this study were obtained from ATCC. Cells were maintained at 37°C in a humidified atmosphere with 5% CO_2. HEK293T and HEK293 cells were grown in Dulbecco's Modified Eagle Medium (DMEM, Invitrogen) which was supplemented with 10% fetal bovine serum (Gibco) and penicillin-streptomycin (Invitrogen). HEK293T and HEK293 cells were confirmed to be free of mycoplasma contamination with the Agilent MycoSensor PCR Assay Kit.

To obtain HEK293 cells stably expressing EYFP, for fluorescent imaging-based studies, cells were co-transfected with EYFP plasmids cloned within a *piggyBac* transposon (pPB bsr2-EYFP) and pCMV-mPBase (mammalian codon-optimized PBase) encoding a piggyBac transposase using Lipofectamine 2000 (Invitrogen) according to the manufacturer's instructions. One day after transfection, the transfected cells were selected with 10 µg/mL of blasticidin (Invitrogen).

Transfections and Drug Selections

24 h prior to transfection, 293T cells were seeded at 40-60% confluency into 24-well plates coated for 30 min with a 0.1 mg/mL solution of poly-D-lysine (MP Biomedicals Inc.) and washed with PBS (Gibco) once prior to media addition. The next day, 500 ng of 3CLpro expression plasmid, unless otherwise stated, was incubated with Opti-MEM and Lipofectamine 2000 for 30 min at room temperature prior to dribbling on cells,

as per manufacturer's protocol. For plating into drug conditions, 20 h after transfection, cells were washed once with PBS and 200 µL Trypsin-EDTA 0.25% (Gibco) was added to cells to release them from the plate. Trypsinized cell slurry was pipetted up and down repeatedly to ensure a single cell suspension. 96-well plates were coated with poly-D-lysine, either coated manually with 1 µg/mL poly-D-lysine in PBS solution for 30 min or purchased pre-coated with poly-D-lysine (Corning). Wells were filled with 100 µL of media ± drug and 1 µg/mL puromycin to select for protease expressing cells and were seeded with 9 µL of trypsinized cell slurry. For data analysis the relative growth in the drug treated condition was compared to the DMSO or lowest drug treated condition to further control for any batch to batch variation in transfection efficiency or other sources of variation between experiments. For higher throughput experiments, multiple individually transfected wells of a 24-well plate were combined after trypsinization and prior to seeding in drug. After seeding into wells containing drug and puromycin, cells were incubated for 48 h unless otherwise specified.

Plasmids

Protease constructs used for compound testing were cloned into the pLEX307 backbone containing a puromycin resistance marker (Addgene #41392) using Gateway LR II Clonase Enzyme mix (Invitrogen). 3CL proteases used in this study were generated using gene fragments ordered from Twist Biosciences. Start codons were added upstream of the P1' (5') serine residue and stop codons were added downstream of the P1 (3') glutamine residue. Sequences were not codon optimized for expression in mammalian cells, but were codon optimized when necessary for synthesis. Inactive 3CL proteases were generated by site directed mutagenesis of the essential catalytic cysteine. DNA was transformed into NEB 10-beta high efficiency competent cells. Sanger sequencing to verify proper inserts were done for all plasmids used in this study (Genewiz).

Plasmid DNA was isolated using standard miniprep buffers (Omega Biotek) and silica membrane columns (Biobasic). To reduce batch-to-batch variability between plasmid DNA isolations and its subsequent impact on transfection efficiency, multiple plasmid DNA extractions were conducted in parallel, diluted to 50 ng/µL and pooled together.

For western blotting, proteases were cloned into the pGCS-N3 backbone which expresses proteases with an N-terminal 3xHA tag (Addgene #85720) using LR II Clonase.

Crystal Violet Staining and Quantification

The crystal violet staining protocol was adapted from Feoktistova et al. [20]. Briefly, after compound incubation with 3CLpro expressing cells in 96-well plates, the medium was discarded and cells were washed once with PBS. Cells were incubated with 50 µL of crystal violet staining solution (0.5% crystal violet in 80% water and 20% methanol) and rocked gently for 30 min. The staining solution was removed and cells were washed four times with water using a multichannel pipette. Stained cells were left to dry for ≥4 h on the

laboratory bench or within the chemical hood (to speed up drying rate). The crystal violet staining solution was eluted by the addition of 200 µL of methanol followed by 30 min of gentle rocking. Plates were sealed with parafilm to mitigate methanol evaporation. 100 µL of eluted stain from each well was transferred to a new 96-well plate for reading in a Tecan Infinite F50 plate reader. Absorbance was measured at 595 nm twice and values were averaged between replicate measurements. Blank wells were included in each batch of experiments, and absorbance values were normalized by background levels of staining from blank wells.

Fluorescence measurements of cell density

Transfected protease expressing cells were plated at ~50% confluency on poly-D-lysine coated 96-well plates (Greiner Bio-OneTM) 48 hours prior to imaging and were washed once immediately before imaging. EYFP fluorescence imaging was performed using an Axio Observer 7 microscope (Zeiss) equipped with a Plan-Apochromat 10X objective (0.45 N.A.) with 1-by-1 pixel binning. Optical Illumination bias was empirically derived by sampling background areas and subsequently used to flatten images. For each well, 9 1.32 mm x 1.32 mm images were taken covering approximately 60% of the well area. After a global background subtraction, cell density was calculated based on area of EYFP intensity. All images were analyzed using custom Matlab scripts.

Western Blotting

For detection of protease expression from HA-tagged protease constructs, 72 h after transfection, HEK293T cells were harvested in RIPA buffer (Alfa Aesar) supplemented with Halt Protease Inhibitor Cocktail on ice (Thermo Scientific). Cells were sonicated for 10 s at 20% amplitude. Sonicated cells were spun at 4°C for 20 min at 12,000 g. Supernatant was collected and protein concentration was normalized to 300 ng/µL supplemented with LDS loading buffer and boiled (Invitrogen). 3 µg of total protein was loaded into a polyacrylamide gel (Invitrogen).

For detection of HA tagged proteases, an HA Tag monoclonal (clone 2-2.2.14; Thermo Scientific catalogue number 26183) antibody was used at a 1:5000 dilution.

Statistical Analysis of Dose Response Curves

For analysis of crystal violet staining experiments, relative growth was calculated from background normalized absorbance values. Test wells containing drug were divided by average background normalized values from wells where cells were expressing protease and exposed to vehicle, when available. Otherwise, values were normalized by values from protease-expressing cells exposed to the lowest concentration of drug included in the dose-response curve. When there were significant deviations from protease-expressing cells exposed to no drug and protease-expressing cells exposed to lowest concentrations of drug included in the dose-response curve, experiments were repeated with normalization by protease-expressing cells

exposed to no drug. CC_{50} values were calculated in Prism using the nonlinear regression functionality and derived from dose-response curves with EYFP transfected cells. A nonlinear curve fitting function accounting for variable curve slopes was calculated by plotting the normalized response as a function of log(compound). Similarly, EC_{50} values were calculated in GraphPad Prism also using the nonlinear regression functionality. A nonlinear curve fitting function measuring the stimulatory response of a compound as a function of an unnormalized response was used to calculate the EC_{50}. All reported values were confirmed to not have ambiguous curve fitting. The 95% confidence interval of EC_{50} calculations was also calculated and included.

For analysis of live virus experiments, EC_{50} values were determined by fitting a nonlinear curve to the data with the assumption of a normalized response (GraphPad Prism). Cells were confirmed as mycoplasma negative prior to use.

Compound Screening

For screening condition optimization, we measured the Z-Factor for replicates of positive controls GC376, tested at 50 μM, and compound 4, tested at 20 μM. Replicate measurements were recorded for DMSO negative controls and positive control compounds after 48, 72, and 96 h of incubation with drug. Background normalized crystal violet absorbance values at each timepoint were collected.

During the drug screen, within each of the four plates screened, two positive controls wells were included to ensure assay reliability, along with several wells with the negative control 0.1% DMSO condition. All compounds were screened at 10 μM resuspended in DMSO (Fisher Scientific).

For hit selection, we employed a robust z-score method. We first normalized data using a robust z-score that uses median and median absolute deviation (MAD) instead of mean and standard deviation. We then used a threshold of 3.5 MAD to determine which drugs rescued the cytotoxicity imposed by expression of the viral protease [49].

Live Virus Assay

The SARS-CoV-2 strain 2019-nCoV/USA_WA1/2020 was grown and titered in Vero-E6 cells. One day before the experiment, Vero-E6 cells were seeded at 30,000 cells/well in 96 well-plates. Serial dilutions of the test compound were prepared in media (EMEM + 10% FCS + penicillin/streptomycin), pipetted onto cells, and virus was subsequently added to each well at an MOI of 0.2. Cells were incubated in a humidified environment at 37 °C with 5% CO_2 for 72 h after addition of virus. Cytopathic effect was scored by visual inspection of the wells performed by researchers that were blinded to the treatment condition. The reported cytopathic effect value represents the average from two independent reviewers. Percent Inhibition was calculated by comparison to control wells with no inhibitor added. All live virus experiments were conducted in a biosafety level 3 lab.

Compounds and Chemical Synthesis

GC376 was purchased from Aobious. Myrecetin, rupintrivir, grazoprevir, saquinavir, fosamprenavir, indinavir, apigenin, quercetin, famotidine, MDL28170, bicailein, betrixaban, and amentoflavone were purchased from Fisher Scientific. Tipranavir was purchased from Cayman Chemical. MAC5576, MAC22272, MAC8120, MAC30731, BTB07404, BTB07408, MWP00332, BTB07417, MWP00508, MWP00333, BTB07407, SPB08384, SPB06613, SPB06636, SPB06591, SPB06593, MWP00709, CC42746, BTB07789, BTB07420, MWP00710, BTB07421, SCR00533, and SEW03089 were purchased from Maybridge. GRL-0496 and GRL-0617 were purchased from Focus Biomolecules. AZVIII-40A (1,2-Benzisothiazol-3(2*H*)-one) was purchased from Alfa Aesar. Other protease inhibitors listed were purchased from TargetMol: Omarigliptin, Apoptosis Activator 2, Picolamine, Muscone, 2-Aminoethanethiol, Dexibuprofen, Glucosamine, Gabexate mesylate, Zalcitabine, Amiloride hydrochloride, Saxagliptin hydrate, Linagliptin, Sitagliptin, Hexylresorcinol, Arbutin, Diminazene Aceturate, 3-Pyridylacetic acid hydrochloride, Racecadotril, Mizoribine, Sodium etidronate, Monobenzone, Limonin, Betulinic acid, PMSF, Fenofibric acid, Ramelteon, Ritonavir, Alogliptin Benzoate, Bortezomib, Acetohydroxamic acid, Nevirapine, Lopinavir, Penciclovir, AOB2796, Maribavir, Trelagliptin succinate, MLN9708, SC514, Ixazomib, Raltegravir potassium, PSI6206, Cilastatin, Taxifolin, Nafamostat mesylate, Daclatasvir dihydrochloride, Darunavir Ethanolate, Ilomastat, Elvitegravir, Dolutegravir sodium, Astragaloside IV, Arctigenin, Stigmasterol, Nobiletin, Celastrol, Glucosamine sulfate, Picroside I, Alvelestat, N-Ethylmaleimide, DAPT, Trelagliptin, Z-VAD(OMe)-FMK, Abietic Acid, Atazanavir sulfate, Abacavir, Balicatib, Carfilzomib, Atazanavir, Vildagliptin, Dapivirine, SB-3CT, PD 151746, PAC1, Camostat mesilate, Efavirenz, Des(benzylpyridyl) Atazanavi, LY2811376, FLI06, SRPIN340, NSC 405020, Leupeptin Hemisulfate, Stearic acid, Epoxomicin, MG101, lavendustin C, BMS707035, Asunaprevir, Loxistatin Acid, GK921, L-685,458, Tenofovir Disoproxil Fumarate, GSK690693, Ledipasvir, ONX0914, PI1840, (+)-Isocorydine hydrochloride, UAMC 00039 dihydrochloride, PE859, RO4929097, Emricasan, CGS 27023A, Talabostat mesylate, Ledipasvir acetone, Batimastat, TOFA, HZ1157, Abacavir sulfate, Sivelestat, Dasabuvir, Calycosin, 4-Methoxysalicylaldehyde, Sebacic acid, Deoxyarbutin, 2-5-dihydroxyacetophenone, Oxyresveratrol, Aloxistatin, Fostemsavir, Tasisulam, Semagacestat, Triciribine, IMR-1A, IMR1, Z-IETD-FMK, VR23, Amprenavir, AA26-9, Dolutegravir, Lomibuvir, Ginsenoside Rh2, UK371804, CA-074 methyl ester, ML281, CP 640186, Hydroumbellic acid, Ethyl gallate, Senegenin, lithospermic acid, Dibenzazepine, LY411575, Paritaprevir, Sofosbuvir, Crenigacestat, Doravirine, Delanzomib, Morroniside, Calycosin-7-O-beta-D-glucoside, Glabridin, Licochalcone A, Velpatasvir, Telaprevir, Odanacatib, Darunavir, Danoprevir, Nelfinavir Mesylate, Oprozomib, AEBSF hydrochloride, Belnacasan, Z-DEVD-FMK, Z-FA-FMK, Trovirdine, MG132, Cabotegravir, and Avagacestat.

See Supplementary Materials and Methods for further information with regard to compounds synthesized for this study.

References

1. Wu F, Zhao S, Yu B, Chen YM, Wang W, Song ZG, Hu Y, Tao ZW, Tian JH, Pei YY, Yuan ML, Zhang YL, Dai FH, Liu Y, Wang QM, Zheng JJ, Xu L, Holmes EC, Zhang YZ. 2020. A new coronavirus associated with human respiratory disease in China. Nature 579, 265–269.

2. Zhou P, Yang XL, Wang XG, Hu B, Zhang L, Zhang W, Si HR, Zhu Y, Li B, Huang CL, Chen HD, Chen J, Luo Y, Guo H, Jiang RD, Liu MQ, Chen Y, Shen XR, Wang X, Zheng XS, Zhao K, Chen QJ, Deng F, Liu LL, Yan B, Zhan FX, Wang YY, Xiao GF, Shi ZL. 2020. A pneumonia outbreak associated with a new coronavirus of probable bat origin. Nature 579, 270–273.

3. Pillaiyar T, Manickam M, Namasivayam V, Hayashi Y, Jung, S. 2016. An Overview of Severe Acute Respiratory Syndrome–Coronavirus (SARS-CoV) 3CL Protease Inhibitors: Peptidomimetics and Small Molecule Chemotherapy. J. Med. Chem. 59, 6595–6628.

4. de Wit E, van Doremalen, N, Falzarano D, Munster VJ. 2016. SARS and MERS: recent insights into emerging coronaviruses. Nat. Rev. Microbiol. 14, 523–534.

5. Berry M, Fielding B, Gamieldien J. 2015. Human coronavirus OC43 3CL protease and the potential of ML188 as a broad-spectrum lead compound: Homology modelling and molecular dynamic studies. BMC Struct. Biol. 15.

6. Huang C, Wei P, Fan K, Liu Y, Lai L. 2004. 3C-like Proteinase from SARS Coronavirus Catalyzes Substrate Hydrolysis by a General Base Mechanism. Biochemistry 43, 4568–4574.

7. Barco A, Feduchi E, Carrasco L. 2000. Poliovirus Protease 3Cpro Kills Cells by Apoptosis. Virology 266, 352–360.

8. Blanco R, Carrasco L, Ventoso I. 2003. Cell Killing by HIV-1 Protease. J. Biol. Chem. 278, 1086–1093.

9. Chau DHW, Yuan J, Zhang H, Cheung P, Lim T, Liu Z, Sall A, Yang D. 2007. Coxsackievirus B3 proteases 2A and 3C induce apoptotic cell death through mitochondrial injury and cleavage of eIF4GI but not DAP5/p97/NAT1. Apoptosis 12, 513–524.

10. Li H, Saucedo-Cuevas L, Yuan L, Ross D, Johansen A, Sands D, Stanley V, Guemez-Gamboa A, Gregor A, Evans T, Chen S, Tan L, Molina H, Sheets N, Shiryaev SA, Terskikh AV, Gladfelter AS, Shresta S, Xu Z, Gleeson JG. 2019. Zika Virus Protease Cleavage of Host Protein Septin-2 Mediates Mitotic Defects in Neural Progenitors. Neuron 101, 1089-1098.e4.

11. Li M, Hsu T, Chen T, Chang S, Lee J, Chen C, Stollar V, Shih S. 2002. The 3C protease activity of enterovirus 71 induces human neural cell apoptosis. Virology 293, 386–395.

12. M'Barek NB, Audoly G, Raoult D, Gluschankof P. 2006. HIV-2 Protease resistance defined in yeast cells. Retrovirology. 3, 58.

13. Weston S, Matthews KL, Lent R, Vlk A, Haupt R, Kingsbury T, Frieman MB. 2019. A yeast suppressor screen used to identify mammalian sirt1 as a proviral factor for middle east respiratory syndrome coronavirus replication. J. Virol. 93, e00197-19.

14. Jin Z, Du X, Xu Y, Deng Y, Liu M, Zhao Y, Zhang B, Li X, Zhang L, Peng, C, Duan Y, Yu J, Wang L, Yang K, Liu F, Jiang R, Yang X, You T, Liu X, Yang X, Bai F, Liu H, Liu X, Guddat LW, Xi W, Xiao G, Qin C, Shi Z, Jiang H, Rao Z, Yang H. 2020. Structure of Mpro from SARS-CoV-2 and discovery of its inhibitors. Nature 582, 289–293.

15. Zhu W, Xu M, Chen CZ, Guo H, Shen M, Hu X, Shinn P, Klumpp-Thomas C, Michael SG, Zheng W. 2020. Identification of SARS-CoV-2 3CL Protease Inhibitors by a Quantitative High-throughput Screening. ACS Pharmacol Transl Sci. 3, 1008-1016.

16. CDC 2020. Information for Laboratories about Coronavirus (COVID-19).

17. Pyrc K, Sims AC, Dijkman R, Jebbink M, Long C, Deming D, Donaldson E, Vabret A, Baric R, van der Hoek, L, Pickles R. 2010. Culturing the Unculturable: Human Coronavirus HKU1 Infects, Replicates, and Produces Progeny Virions in Human Ciliated Airway Epithelial Cell Cultures. J. Virol. 84, 11255–11263.

18. Sacco MD, Ma C, Lagarias P, Gao A, Townsend JA, Meng X, Dube P, Zhang X, Hu Y, Kitamura N, Hurst B, Tarbet C, Marty MT, Kolocouris A, Xiang Y, Chen Y, Wang J. 2020. Structure and inhibition of the SARS-CoV-2 main protease reveals strategy for developing dual inhibitors against Mpro and cathepsin L. Sci. Adv. 6, eabe0751.

19. Sies H, Parnham MJ. 2020. Potential therapeutic use of ebselen for COVID-19 and other respiratory viral infections. Free Radic. Biol. Med. 156, 107–112.

20. Feoktistova M, Geserick P, Leverkus M. 2016. Crystal Violet Assay for Determining Viability of Cultured Cells. Cold Spring Harb. Protoc. 4, pdb.prot087379.

21. Ma C, Sacco MD, Hurst B, Townsend JA, Hu Y, Szeto T, Zhang X, Tarbet B, Marty MT, Chen Y, Wang J. 2020. Boceprevir, GC-376, and calpain inhibitors II, XII inhibit SARS-CoV-2 viral replication by targeting the viral main protease. Cell Res. 1–15.

22. Froggatt HM, Heaton BE, Heaton NS. 2020. Development of a fluorescence based, high-throughput SARS-CoV-2 $3CL^{pro}$ reporter assay. J. Virol. JVI.01265-20.

23. Hung H, Ke Y, Huang SY, Huang P, Kung Y, Chang T, Yen K, Peng T, Chang S, Huang C, Tsai Y, Wu S, Lee S, Lin J, Liu B, Sung W, Shih S, Chen C, Hsu J. 2020. Discovery of M Protease Inhibitors Encoded by SARS-CoV-2. Antimicrob. Agents Chemother. 64, e00872-20.

24. Iketani S, Forouhar F, Liu H, Hong SJ, Lin F, Nair MS, Zask A, Huang Y, Xing L, Stockwell, BR, Chavez A, Ho DD. 2021. Lead compounds for the development of SARS-CoV-2 3CL protease inhibitors. Nat. Commun. 12, 2016.

25. Luan X, Shang W, Wang Y, Yin W, Jiang Y, Feng S, Wang Y, Liu M, Zhou R, Zhang Z, Wang F, Cheng W, Gao M, Wang H, Wu W, Tian R, Tian Z, Jin Y, Jiang H, Zhang L, Xi HE, Zhang S. 2020. Structure Basis for Inhibition of SARS-CoV-2 by the Feline Drug GC376. BioRxiv 2020.06.07.138677.

26. Vuong W, Khan MB, Fischer C, Arutyunova E, Lamer T, Shields J, Saffran HA, McKay RT, van Belkum MJ, Joyce MA, Young HS, Tyrrell DL, Vederas JC, Lemeieux MJ. 2020. Feline coronavirus drug inhibits the main protease of SARS-CoV-2 and blocks virus replication. Nat. Commun. 11, 4282.

27. Dai W, Zhang B, Jiang X, Su H, Li J, Zhao Y, Xie X, Jin Z, Peng J, Liu F, Li C, Li Y, Bai F, Wang H, Cheng X, Cen X, Hu S, Yang X, Wang J, Liu X, Xiao G, Jiang H, Rao Z, Zhang L, Xu Y, Yang H, Liu H. 2020. Structure-based design of antiviral drug candidates targeting the SARS-CoV-2 main protease. Science 368, 1331–1335

28. Yang S, Chen SJ, Hsu MF, Wu JD, Tseng CT, Liu YF, Chen HC, Kuo CW, Wu CS, Chang LW, Chen WC, Liao SY, Chang TY, Hung HH, Shr HL, Liu CY, Huang YA, Chang LY, Hsu JC, Peters CJ, 28. Wang AH, Hsu MC. 2006. Synthesis, Crystal Structure, Structure−Activity Relationships, and Antiviral Activity of a Potent SARS Coronavirus 3CL Protease Inhibitor. J. Med. Chem. 49, 4971–4980.

29. Ghosh AK, Gong G, Grum-Tokars V, Mulhearn DC, Baker SC, Coughlin M, Prabhakar BS, Sleeman K, Johnson ME, Mesecar AD. 2008. Design, synthesis and antiviral efficacy of a series of potent chloropyridyl ester-derived SARS-CoV 3CLpro inhibitors. Bioorg. Med. Chem. Lett. 18, 5684–5688.

30. Ma C, Hu Y, Townsend JA, Lagarias P, Marty MT, Kolocouris A, Wang J. 2020. Ebselen, disulfiram, carmofur, PX-12, tideglusib, and shikonin are non-specific promiscuous SARS-CoV-2 main protease inhibitors. BioRxiv. 2020.09.15.299164.

31. Seale LA, Torres DJ, Berry MJ, Pitts MW. 2020. A role for selenium-dependent GPX1 in SARS-CoV-2 virulence. Am. J. Clin. Nutr. 112, 447-448.

32. Węglarz-Tomczak E, Tomczak JM, Talma M, Burda-Grabowska M, Giurg M, Brul S. 2021 Identification of ebselen and its analogues as potent covalent inhibitors of papain-like protease from SARS-CoV-2. Sci. Rep. 11, 3640.

33. Zmudzinski M, Rut W, Olech K, Granda J, Giurg M, Burda-Grabowska M, Zhang L, Sun X, Lv Z, Nayak D, Kesik-Brodacka M, Olsen SK, Hilgenfeld R, Drag M. 2020. Ebselen derivatives are very potent dual inhibitors of SARS-CoV-2 proteases - PL^{pro} and M^{pro} in in vitro studies. BioRxiv 2020.08.30.273979.

34. Kim Y, Liu H, Kankanamalage ACG, Weerasekara S, Hua DH, Groutas WC, Chang K, Pedersen NC. 2016. Reversal of the Progression of Fatal Coronavirus Infection in Cats by a Broad-Spectrum Coronavirus Protease Inhibitor. PLOS Pathog. 12, e1005531.

35. Zhang J, Chung TDY, Oldenburg KR. 1999. A Simple Statistical Parameter for Use in Evaluation and Validation of High Throughput Screening Assays. J. Biomol. Screen. 4, 67–73.

36. Birmingham A, Selfors LM, Forster T, Wrobel D, Kennedy CJ, Shanks E, Santoyo-Lopez J, Dunican, DJ, Long, A, Kelleher, D, Smith Q, Beijersbergen RL, Ghazal P, Shamu CE. 2009. Statistical Methods for Analysis of High-Throughput RNA Interference Screens. Nat. Methods 6, 569–575.

37. Kim Y, Lovell S, Tiew K, Mandadapu SR, Alliston KR, Battaile KP, Groutas WC, Chang K. 2012. Broad-Spectrum Antivirals against 3C or 3C-Like Proteases of Picornaviruses, Noroviruses, and Coronaviruses. J. Virol. 86, 11754–11762.

38. Blanchard JE, Elowe NH, Huitema C, Fortin PD, Cechetto JD, Eltis LD, Brown ED. 2004. High-throughput screening identifies inhibitors of the SARS coronavirus main proteinase. Chem. Biol. 11, 1445–1453.

39. Binford SL, Weady PT, Maldonado F, Brothers MA, Matthews DA, Patick AK. 2007. In vitro resistance study of rupintrivir, a novel inhibitor of human rhinovirus 3C protease. Antimicrob. Agents Chemother. 51, 4366–4373.

40. Patick AK, Binford SL, Brothers MA, Jackson RL, Ford CE, Diem MD, Maldonado F, Dragovich PS, Zhou R, Prins TJ, Fuhrman SA, Meador JW, Zalman LS, Matthews DA, Worland ST. 1999. In vitro antiviral activity of AG7088, a potent inhibitor of human rhinovirus 3C protease. Antimicrob. Agents Chemother. 43, 2444–2450.

41. Ratia K, Pegan S, Takayama J, Sleeman K, Coughlin M, Baliji S, Chaudhuri R, Fu W, Prabhakar BS, Johnson ME, Baker SC, Ghosh AK, Mesecar AD. 2008. A noncovalent class of papain-like protease/deubiquitinase inhibitors blocks SARS virus replication. Proc. Natl. Acad. Sci. 105, 16119.

42. Coelho AC, García Díez J. 2015. Biological Risks and Laboratory-Acquired Infections: A Reality That Cannot be Ignored in Health Biotechnology. Front. Bioeng. Biotechnol. 3, 56.

43. Klotz LC, Sylvester EJ 2014. The Consequences of a Lab Escape of a Potential Pandemic Pathogen. Front. Public Health 2.

44. Wei J, Alfajaro MM, DeWeirdt PC, Hanna RE, Lu-Culligan WJ, Cai WL, Strine MS, Zhang SM, Graziano VR, Schmitz CO, Chen JS, Mankowski MC, Filler RB, Ravindra NG, Gasque V, de Miguel FJ, Patil A, Chen H, Oguntuyo KY, Abriola L, Surovtseva YV, Orchard RC, Lee B, Lindenbach BD, Politi K, van Dijk D, Kadoch C, Simon MD, Yan Q, Doench JG, Wilen CB. (2020). Genome-wide CRISPR Screens Reveal Host Factors Critical for SARS-CoV-2 Infection. Cell. 184, 76-91.

45. Jeon S, Ko M, Lee J, Choi I, Byun SY, Park S, Shum D, Kim S. 2020. Identification of Antiviral Drug Candidates against SARS-CoV-2 from FDA-Approved Drugs. Antimicrob. Agents Chemother. 64, e00819-20.

46. Dittmar M, Lee JS, Whig K, Segrist E, Li M, Kamalia B, Castellana L, Ayyanathan K, Cardenas-Diaz FL, Morrisey EE, Truitt R, Yang W, Jurado K, Samby K, Ramage H, Schultz DC, Cherry S. 2021. Drug repurposing screens reveal cell-type-specific entry pathways and FDA approved drugs active against SARS-Cov-2. Cell Rep. 6, 108959.

47. Kilianski A, Mielech A, Deng X, Baker SC. 2013. Assessing activity and inhibition of MERS-CoV papain-like and 3C-like proteases using luciferase-based biosensors. J. Virol. 87:11955–11962.

48. O'Brien A, Chen D, Hackbart M, Close BJ, O'Brien TE, Saeed M, Baker SC. 2021. Detecting SARS-CoV-2 3CLpro expression and activity using a polyclonal antiserum and a luciferase-based biosensor. Virology. 556, 73-78.

49. Iglewicz B, Hoaglin DC. 1993. How to detect and handle outliers. ASQC Quality Press.

Acknowledgements

Compound 11a was synthesized and generously provided by Shi-Xian Deng, Columbia University. This work was supported by a grant from the Jack Ma Foundation to D.D.H. and A.C. and by grants from Columbia Technology Ventures and the Columbia Translational Therapeutics (TRx) program to B.R.S. Further support for these studies comes from a pilot grant award from the Herbert Irving Comprehensive Cancer Center in partnership with the Irving Institute for Clinical and Translational Research at Columbia University to H.Y. and A.C. A.C. is also supported by a Career Awards for Medical Scientists from the Burroughs Wellcome Fund. S.J.R is supported by NIH grant F31NS111851. S.I. is supported by NIH grant T32AI106711.

Author contributions

S.J.R., S.I, and A.C conceived the project. S.J.R., S.I., B.R.S., D.D.H., and A.C. planned and designed the experiments. S.J.R. performed crystal violet-based assays. S.J.R. and S.K. performed the HEK293-EYFP based assays. S.J.R., S.I., and S.J.H. cloned plasmids. A.Z. and H.L. synthesized compounds and provided compound structure information for synthesized compounds. N.E.S.T. and T.R. synthesized compounds NT-1-21, NT-1-24, and NT-1-32. S.L. and T.R. synthesized compound SL-4-241. M.S.N. and Y.H. conducted the live virus assays. F.L. and L.X. conducted structural modeling and chemical composition analysis. S.K. and H.Y. performed imaging and created the HEK293-EYFP cell line. S.J.R. and S.M. conducted data analysis. S.J.R, S.I., S.J.H, and A.C. wrote the manuscript with input from all authors.

Competing interests

S.I., H.L., A.Z., B.R.S., A.C., and D.D.H. are inventors on a patent application submitted based on some of the molecules described in this work. B.R.S. is an inventor on additional patents and patent applications related to small molecule therapeutics, and co-founded and serves as a consultant to Inzen Therapeutics and Nevrox Limited.

Data and materials availability

All reagents generated in this study are without restriction. Plasmids generated in this study will be deposited to Addgene. Source data for all figures are provided with this manuscript online. All statistics were performed using Prism v.8.4.2.

651 **Figures and Tables**

652 **Table 1. Comparison of literature reported live virus based EC_{50} values compared to values**
653 **generated during this study.** CPE = Cytopathic effect.

Protease	Drug	Calculated EC_{50} (μM)	Literature Reported Value (μM)	Method	Cell Line	Citation
SARS-CoV-2 3CLpro	GC376	3.3	3.4	CPE	Vero E6	Ma et al. [21]
			0.9	Plaque Assay	Vero E6	Vuong et al. [26]
			0.18	qPCR	Vero E6	Luan et al. [25]
			2.2	qPCR	Vero E6	Froggatt et al. [22]
			4.5	CPE	Vero E6	Iketani et al. [24]
SARS-CoV-2 3CLpro	11a	6.89	3.8	CPE	Vero E6	This study
			0.5	Plaque Assay	Vero E6	Dai et al. [27]
SARS-CoV-2 3CLpro	compound 4	0.98	3.0	CPE	Vero E6	Iketani et al. [24]
SARS-CoV-2 3CLpro	GRL-0496	5.05	9.1	CPE	Vero E6	This study
SARS-CoV 3CLpro	GRL-0496	7.84	6.9	CPE	Vero E6	Ghosh et al. [29]
SARS-CoV-2 3CLpro	GC373	2.8	1.5	Plaque Assay	Vero E6	Vuong et al.
			4.8	CPE	Vero E6	This Study
SARS-CoV PLP	GRL-0617	5.65	14.5	CPE	Vero E6	Ratia et al. [41]
HRV-B14 3Cpro	Rupintrivir	0.0086	0.021	CPE	H1-HeLa	Binford et al. [39]
			0.013	CPE	H1-HeLa	Patick et al. [40]

654

Fig. 1. Expression of SARS-CoV-2 3CLpro in HEK293T cells results in toxicity that can be rescued by the protease inhibitor GC376. a. SARS-CoV-2 3CL toxicity is dependent on protease activity and can be visualized with crystal violet staining. C145A represents the catalytically null variant of the protease. **b**. Quantification of crystal violet staining in a. **c.** Detection of protease expression via western blotting. **d**. Treatment of SARS-CoV-2 3CLpro expressing cells with protease inhibitor GC376 results in rescue of cytotoxicity. **e**. Quantification of d. Data are shown as mean ± s.d. for four technical replicates.

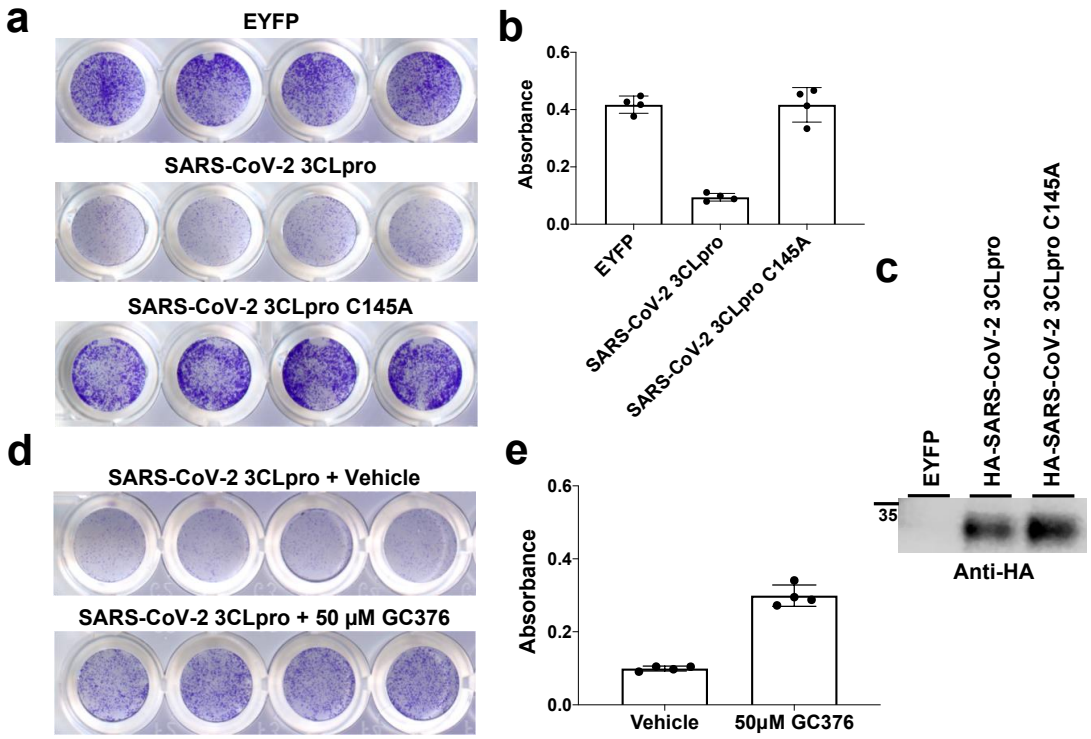

Fig. 2. Dose response curves for SARS-CoV-2 3CLpro can be conducted with transfection-based assays. a-c. SARS-CoV-2 3CLpro can be inhibited by known 3CLpro inhibitors GC376, compound 4, and 11a. The toxicity of each compound was determined by treating EYFP-transfected cells with indicated concentrations of drug and is reported as Cell Viability. **d.** Chemical structures for each of the compounds tested. EC_{50} values are displayed as best-fit value alongside 95% confidence interval. CC_{50} values are displayed as best-fit value. Data are shown as mean ± s.d. for four technical replicates.

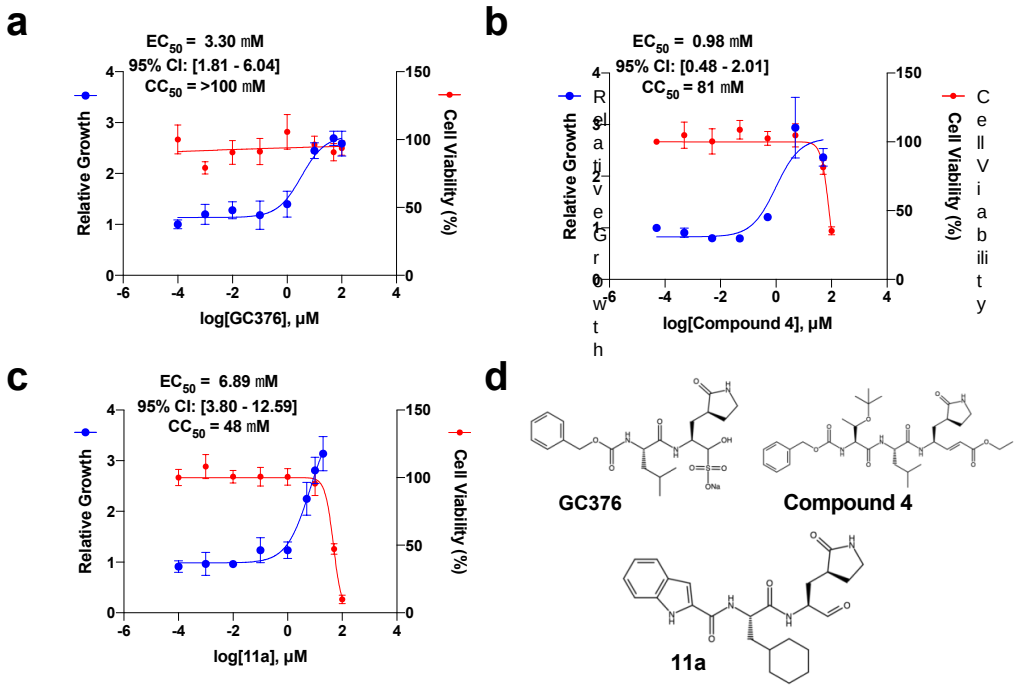

Fig. 3. The activity of GC376, compound 4, and 11a show variable effectiveness and potency against the coronavirus 3CL proteases from SARS-CoV, MERS-CoV, Bat-CoV-HKU9, HCoV-NL63, and IBV. EC_{50} values are displayed as best-fit value alongside 95% confidence interval. CC_{50} values are displayed as best-fit value. Data are shown as mean ± s.d. for three or four technical replicate

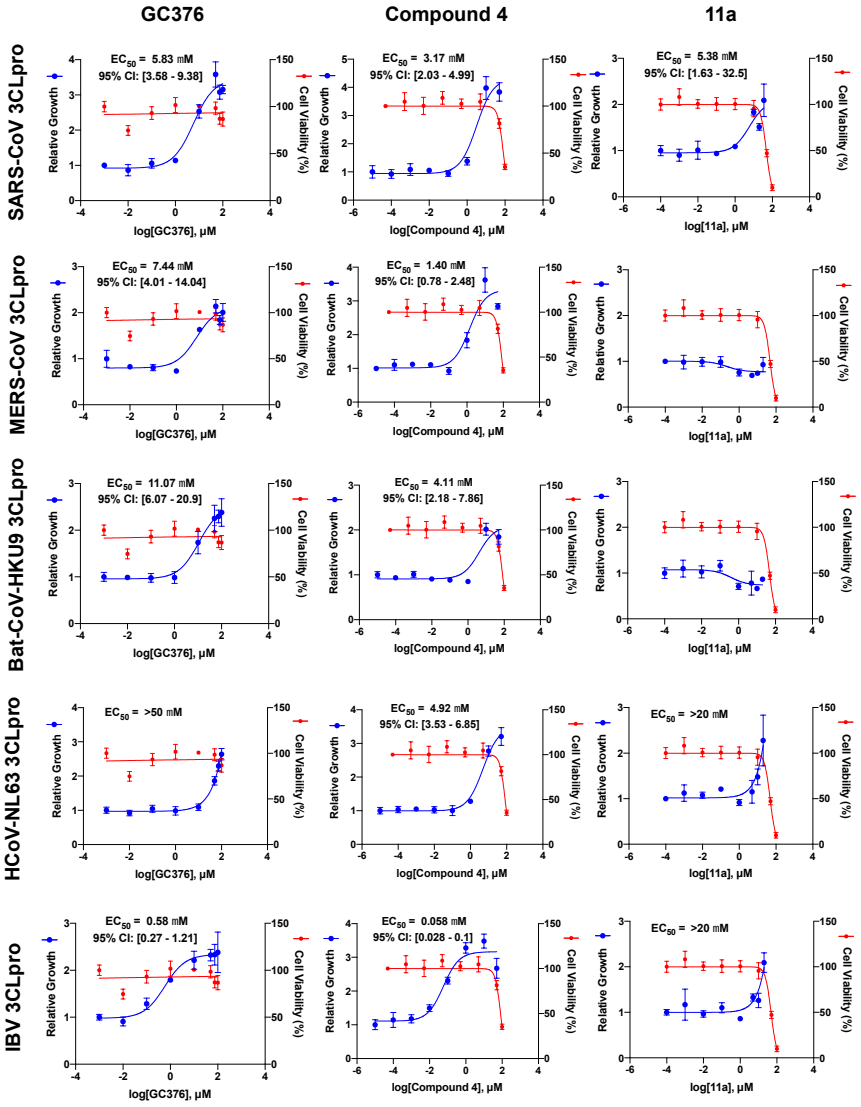

Fig. 4. Structural differences between SARS-CoV-2 3CLpro and MERS-CoV 3CLpro determine sensitivity to compounds containing large P2 substituents. a. Structure of SARS-CoV-2 3CLpro (PDB: 6LZE). **b.** Structure of MERS-CoV 3CLpro (PDB: 5WKJ). **c.** Structure of GC376 analog SL-4-241 containing a P2 cyclohexylmethyl substituent. **d.** Dose-response profiling and cytotoxicity determination of SL-4-241 against the SARS-CoV-2 3CLpro. **e.** Dose-response profiling and cytotoxicity determination of SL-4-241 against the MERS-CoV 3CLpro. Data are shown as mean ± s.d. for four technical replicates.

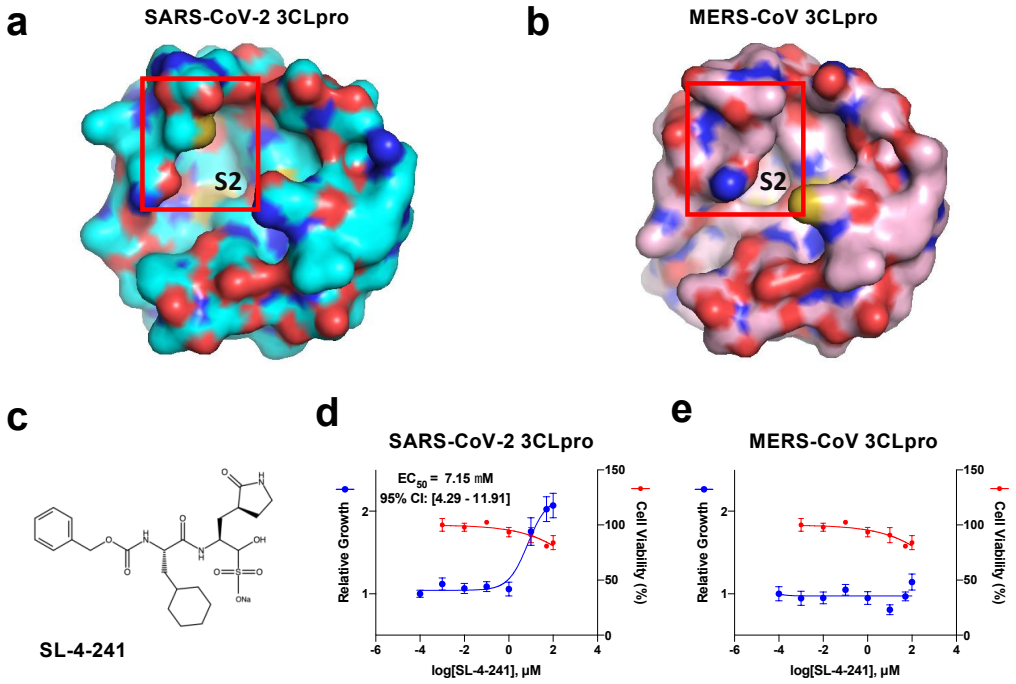

Fig. 5. Small-scale drug screen and structure-activity profiling at 10 μM identify two compounds, GC373 and GRL-0496, with activity against the SARS-CoV-2 3CLpro. a. Identification of hits from the drug screen and structure-activity profiling. Positive control compounds were included in each plate and are highlighted. **b**. Compounds with structural similarity to known inhibitors. Compounds in bold are molecules that show activity against the SARS-CoV-2 3CLpro at 10 μM. **c**. Dose-response profiling and cytotoxicity determination of GRL-0496 against the SARS-CoV-2 3CLpro. **d**. Live virus testing of GRL-0496 against SARS-CoV-2. EC_{50} values are displayed as best-fit value alongside 95% confidence interval. The live virus assay was conducted with two biological replicates, each with three technical replicates and the EC_{50} value was derived from all replicates. CC_{50} values are displayed as best-fit value. Data are shown as mean ± s.d. for three or four technical replicates.

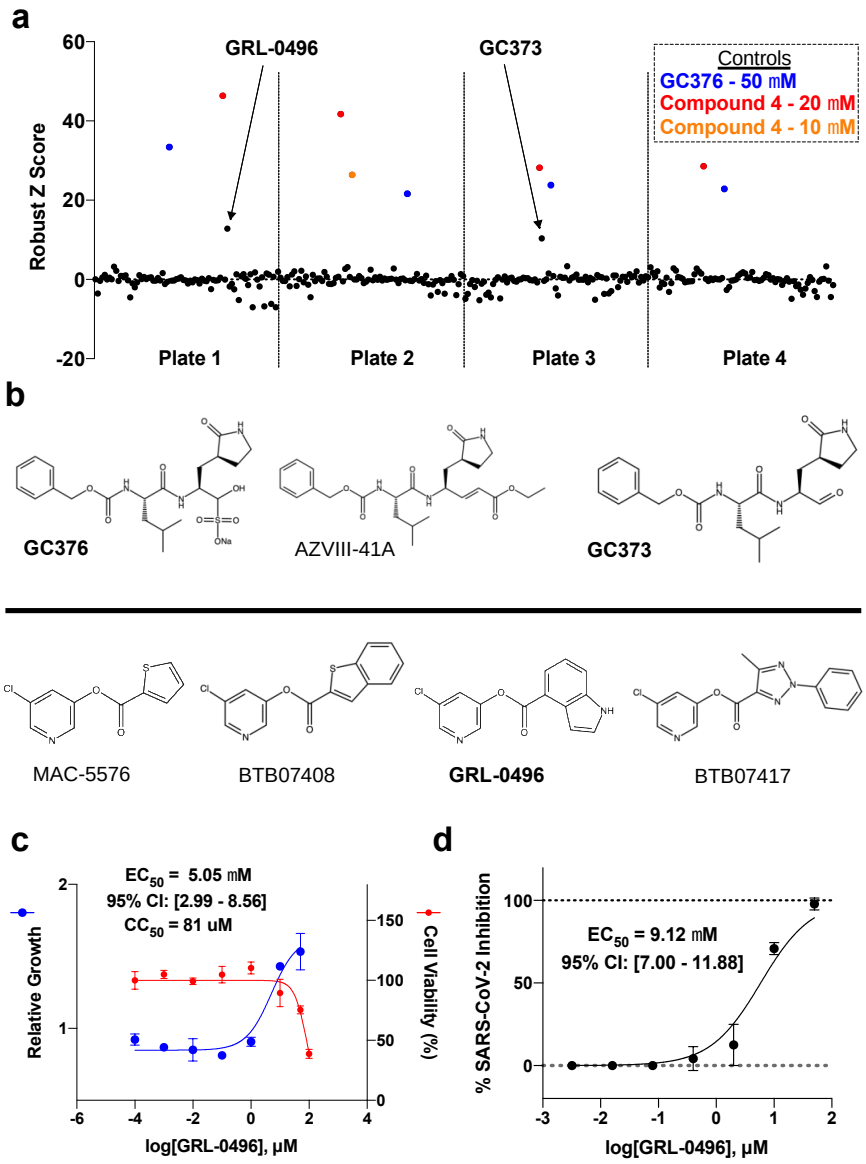

693
694

Fig. 6. Compound 4 and GC376 are broadly active 3CL protease inhibitors. EC_{50} values are displayed as best-fit value alongside 95% confidence interval. Data are shown as mean ± s.d. for four technical replicates. The genus from which each coronavirus is derived is listed below each protease's name.